DEPOSITION OF NIOBIUM AND OTHER SUPERCONDUCTING MATERIALS WITH HIGH POWER IMPULSE MAGNETRON SPUTTERING: CONCEPT AND FIRST RESULTS*

André Anders#, Rueben J. Mendelsberg, Sunnie Lim, Matthijs Mentink, Jonathan L. Slack, and Joseph G. Wallig, Lawrence Berkeley National Laboratory, Berkeley, California, U.S.A.
Alexander V. Nollau, University of the German Armed Forces, Neubiberg, Germany
Georgy Yu. Yushkov, High Current Electronics Institute, Tomsk, Russia

Abstract

Niobium coatings on copper cavities have been considered as a cost-efficient replacement of bulk niobium RF cavities, however, coatings made by magnetron sputtering have not quite lived up to high expectations due to *Q*-slope and other issues. High power impulse magnetron sputtering (HIPIMS) is a promising emerging coatings technology which combines magnetron sputtering with a pulsed power approach. The magnetron is turned into a metal plasma source by using very high peak power density of ~ 1 kW/cm^2. In this contribution, the cavity coatings concept with HIPIMS is explained. A system with two cylindrical, movable magnetrons was set up with custom magnetrons small enough to be inserted into 1.3 GHz cavities. Preliminary data on niobium HIPIMS plasma and the resulting coatings are presented. The HIPIMS approach has the potential to be extended to film systems beyond niobium, including other superconducting materials and/or multilayer systems.

INTRODUCTION

The common approach to superconducting radio frequency (SRF) cavities is using bulk niobium, a proven technology [1, 2]. Niobium, a type II superconductor, is the material of choice for its high critical temperature (T_c = 9.2 K) and its high superheating critical magnetic field, which is of the order of the thermodynamic critical field (H_c = 2000 Oe). Well prepared niobium SRF cavities can have electric fields exceeding 20 MV/m with a quality factor Q of the order 10^{10}. Cavities capable of higher field strength and with higher quality factor have been made, although Q generally decreases as the field is pushed to the limits of breakdown and quenching.

The cost of niobium is high, especially high purity material qualified to have a high residual resistivity ratio (RRR, of order 300). Making the cavities of bulk niobium may be prohibitively expensive for high energy linacs that make use of 650 MHz or lower, implying large cavities. A possible approach is to move to niobium coatings, reducing the need for niobium to a tiny fraction [3]. The idea is not new [4, 5]: the LEP-II accelerator at CERN used 288 4-cell cavities at 352.2 MHz, 256 of which were Nb-coated copper cavities. The niobium was deposited using sputtering from a cylindrical magnetron inserted into the cleaned, electropolished, and outgassed copper cavities [6]. Although the accelerator was a success, the performance of the cavities was limited by a significant *Q*-slope: the quality factor drops significantly at high fields. High fields are highly desirable (a) to make a linear accelerator as short and cost-effective as possible, or (b) to obtain the highest energy from a circular machine. Although the details of the *Q*-slope and film structure are still subject to investigations [7], it is clear that an improved film deposition method is needed to achieve higher quality coatings.

A possible approach using energetic deposition from the plasma phase has been investigated for some years using (filtered) cathodic vacuum arcs [8-10]. Very encouraging are recent results where niobium films of RRR = 77 [10] and even 300 [11] were produced, though those record values were obtained for hot sapphire substrates, not cavities. A new energetic deposition technology is high power impulse magnetron sputtering (HIPIMS) [12], also known as high power pulsed sputtering (HPPMS). In this contribution, the concept of using HIPIMS for SRF cavities is explored and some very preliminary results are reported.

HIGH POWER IMPULSE MAGNETRON SPUTTERING

HIPIMS is an emerging technology that combines conventional magnetron sputtering with a pulsed power approach [13-15]. The process is pulsed with a power density at the target surface during the pulse exceeding the typical dc power density by about two orders of magnitude. This implies that the off-time between pulses is long, and the duty cycle is only of order 1%. It is becomes increasingly common to use the term “impulse” to distinguish the process from lower power pulsed sputtering. The most important result of the very significant increase of power is the ionization of the sputtered atoms. The newly formed target ions participate in the sputtering process, i.e. self-sputtering is important. Ionization of the sputtered material delivers energy and momentum to the growing film on a substrate, which greatly affects density and texture of the film. For example, this has been studied for tantalum films, where it was shown that the HIPIMS process leads to smooth films of well aligned grains with their c-axes normal to the surface [16]. A low resistivity bcc phase could be

*This work was initially supported by an LDRD grant by Lawrence Berkeley National Laboratory, and later by the Office of High Energy Physics, U.S. Department of Energy, under Contract No. DE-AC02-05CH11231.

#aanders@lbl.gov

obtained even for non-normal flow of plasma to the surface [17].

To understand the effect we should recall that a space charge layer, a sheath, is established between plasma and a surface, and the voltage drop in the sheath gives rise to an additional contribution to the energy of an ion upon arrival, as described by the equation [18]

$$E_i = E_{i0} + Q_{CS} e V_{sheath},$$

where E_{i0} is the kinetic energy of the ion in the plasma, i.e. before acceleration in the sheath, Q_{CS} is the charge state number, e is the elementary charge, and V_{sheath} is the voltage drop in the sheath, assuming that the wall's surface potential is more negative with respect to the plasma potential.

A flow of ionized species from the magnetron, as opposed to a flow of sputtered neutral atoms, thus allows us to influence the kinetic energy of film-forming particles, which is best utilized if a bias is applied to the substrate. Acceleration in the sheath not only changes the energy but also the direction of the ions' trajectories, which will be illustrated later.

Energetic deposition can be achieved via a number of distinct i-PVD (ionized physical vapor deposition) technologies, most notably cathodic arc deposition [19], pulsed laser deposition [20], magnetron deposition with supplemental RF discharge ionization [21], and more recently, HIPIMS. i-PVD can be coupled to pulsed biasing techniques also known as Plasma Immersion Ion Implantation and Deposition (PIII&D) [22]. Among i-PVD techniques, HIPIMS is attractive because no additional components like RF coils are needed, and unlike with laser ablation and cathodic arcs, no macroparticles are produced (caveat: should unwanted "arcing" occur on the magnetron target, macroparticles are produced and therefore a modern power supply with very fast arc suppression is required).

The fact that a fraction of the sputtered atoms is ionized, and that ions return to the target, causing self-sputtering, implies that less film-forming particles arrive at the substrate compared to dc sputtering at equal average power. In other words, HIPIMS has a lower average deposition rate compared to dc sputtering [23] - an issue much discussed for its economic implications. Here, when making high purity niobium films, the rate issue is of concern in terms of incorporation of residual gas in the growing film. A relatively lower flux of metal compared to the flux of residual gas suggests that more impurities are incorporated. The issue is a bit more complicated, though, since the deposition occurs in pulses, where the rate during the pulse far exceeds the dc rate. It is conceivable that the contamination from the background appears in a nanometer-size multilayer structure provided that each pulse increases the film thickness by nanometer steps. For thinner coatings per pulse, one could expect uniform, well-dispersed contamination. In any case, it is expected that UHV or UHV-like conditions are needed.

EXPERIMENTAL SETUP

Two vacuum chambers at Berkeley Lab are equipped with HIPIMS technology. We will first focus on the first, general-use chamber where samples for preliminary test have been deposited. Later we will describe a new chamber dedicated to SRF cavity coatings.

HIPIMS in the General-use Chamber

The general-use deposition chamber has a base pressure in the low 10^{-5} Pa range. It is equipped with a 2" (5 cm) unbalanced magnetron connected to an SPIK2000A power supply (Melec) upgraded to peak currents up to 500 A. An outline of the chamber is shown in Fig. 1. Process gas (argon or krypton) is supplied via mass flow controllers; the pressure is monitored by a capacitance gauge (Baratron by MKS). The pumping speed can be adjusted using an adjustable gate valve. The substrate's temperature can be raised up to 400°C using a radiative heater, and the temperature can be measured using a K-type thermocouple and an infrared temperature sensor (Raytek).

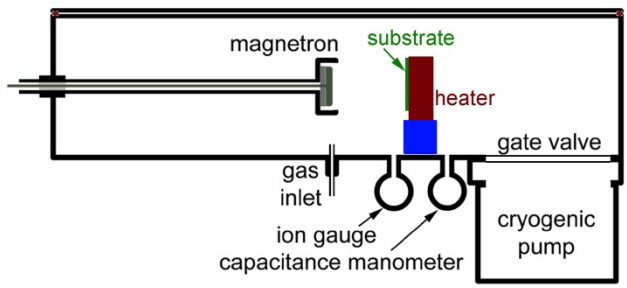

Figure 1: Schematic of the HIPIMS setup of the general-use chamber; this is a side-view cross section of the cylindrical stainless steel chamber having a diameter of 1 meter.

The maximum applied voltage to the target is 1000 V, with a selectable pulse duration typically between 10 μs and 1 ms. The large capacitor bank (0.072 F) in the supply ensures constant voltage mode during the pulse, with the current adjusting itself depending on the plasma impedance.

Depending on the applied voltage, gas pressure, magnetic field strength and other parameters, the HIPIMS discharge may remain in a relative modest power mode, or the discharge current may rapidly run away, typically within less than 100 μs, to a high-current, high-power mode. This has been extensively documented in the literature [14, 24], including for niobium targets [15].

To illustrate the discharge dynamics and variety of plasma impedances, long pulses of 1 ms can be used. Figures 2 and 3 show examples of runaway behavior to high currents which can be observed once a certain voltage threshold is reached.

Despite higher costs, krypton (atomic mass 83.3) may be preferable to argon (atomic mass 40) as the sputter gas for two reasons: (i) krypton is less trapped in the niobium film than argon, and (ii) krypton tends to damp plasma

instabilities. The last argument is clearly visible by looking at the oscillations and "noise" seen in the high current traces of Figs. 1 and 2. HIPIMS plasmas exhibit a range of instabilities with different characteristic frequencies. While some instabilities can be harmful to the power supply and could disrupt the process, other instabilities are actually needed for the HIPIMS discharge to work. For example, Brenning and coworkers [25] found that instabilities are responsible for an anomalously high cross-magnetic field transport of electrons.

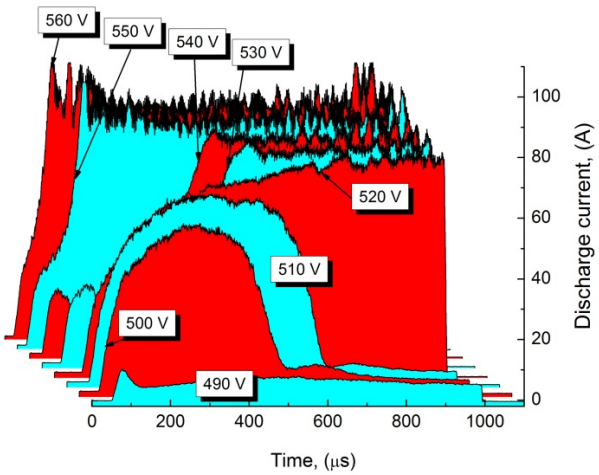

Figure 2: HIPIMS current pulses for a 2" niobium target operating in 0.5 Pa of argon; the applied target voltage is shown as a parameter.

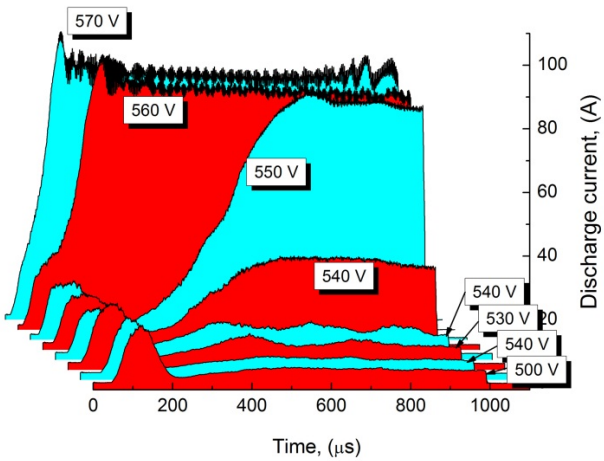

Figure 3: As figure 1 but with krypton as sputter gas. For more details see Ref. [15].

The current curves in figures 2 and 3 show a characteristic first peak that is associated with gas rarefaction [26], a reduction of gas density due to the flux of sputtered atoms or 'sputter wind', which is very strong under HIPIMS conditions [27]. For conditions below the runaway threshold (i.e. at relatively low applied voltage), the discharge currents settles at low voltage, not much different than in ordinary dc discharges, except we terminate the discharge after 1 ms. At a threshold, which is typically in the range 530-540 V, the discharge runs away to a high current level. This new mode is largely characterized by metal self-sputtering, as it is evident by optical emission spectroscopy [28] and particle spectrometry using a plasma analyzer like the HIDEN EQP 300 [29]. The general-use chamber, Fig. 1, is equipped with such analyzer (not shown), which represents a combined energy analyzer and quadrupole mass spectrometer.

Initial HIPIMS deposition of Nb was done on copper coupons, following the research that has been done on sputtered Nb on copper cavities. Serendipitously it was found that the niobium films stuck much better to the aluminum substrate holder than to the copper coupons. Apparently, the native aluminum oxide layer acts like an adhesion layer between the metallic aluminum and the niobium film. This suggested to consider cavities of aluminum and to treat the aluminum substrate in order to form an intentional oxide layer prior to being coated with niobium. Aluminum would have the additional advantage of lower material cost than copper, and relative ease of machining and forming. However, the vast experience of making RF cavities from copper at CERN, Fermi Lab and other places would not be fully applicable, and other issues should be expected. Much of the exploration reported here focused on making niobium films on aluminum substrates having an aluminum oxide surface.

Dedicated SRF Deposition Chamber

In parallel to performing exploratory experiments in the general-use chamber, a new, cleaner, dedicated deposition chamber was designed and built. In order to process actual cavities, a set of two, movable cylindrical magnetrons was used. Their size was selected such as to deposit films on 1.3 GHz cavities. The two magnetrons were mounted on movable arms, as shown in Fig. 4, to uniformly coat the inside of the cavity while slowly traveling through it.

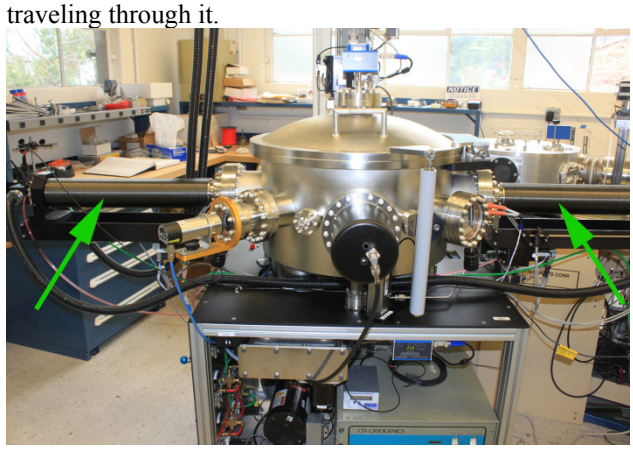

Figure 4: Deposition chamber dedicated to the coating of 1.3 GHz cavities with niobium using the HIPIMS process. The cylindrical magnetrons are mounted on opposing arms, indicated by the arrows, which allows them to slowly move in a synchronized manner driven by computer-controlled stepper motors.

The idea of using two magnetrons is mostly driven by the desire of having the option of biasing the cavities, where the bias is one of the main parameters for film optimization. If there was only one magnetron, as

indicated in Figure 5, one would conveniently use the cavity as the anode for the HIPIMS process (unless a dedicated anode is provided). When using two magnetrons, Fig. 6, one can employ the dual magnetron concept were on target serves as the cathode, and the other as the anode. The polarity of the targets is alternated at a frequency typical for HIPIMS, such a 100 Hz. As a result, the cavity does not participate in the discharge process and can be biased at will, using another, independent power supply. Additionally, the deposition rate can be doubled each by using each of the magnetrons at its maximum power rating. This leads to shorter process time and reduced incorporation of residual gas contaminants.

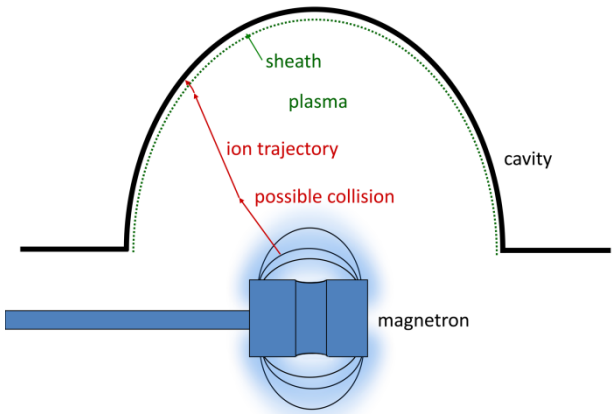

Figure 5: Schematic of a cylindrical magnetron in a cavity (the arched lines indicate the magnetic field with the erosion "racetrack" forming beneath). When the cavity is used as the anode of the discharge, the sheath voltage is not independently available as a process parameter.

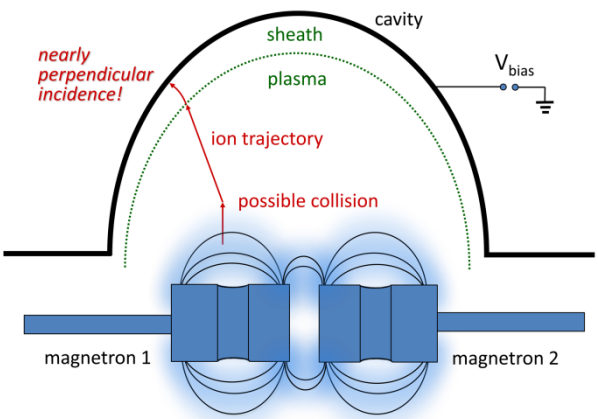

Figure 6: Schematic of a dual magnetron setup: here, the cavity can be biased and the sheath can be used to control the ion energy and ion impact angle.

The cavity bias can be done in dc mode or pulsed, where the latter gives us more parameters to adjust besides the bias amplitude, namely the bias pulse length and duty cycle. Using cathodic arc plasmas, such optimization of pulsed bias was shown to enable conformal coating and filling of sub-micrometer features [19, 30].

PRELIMINARY RESULTS

An experiment was carried out in the general-use chamber to explore the possibility of "gasless" self-sputtering of niobium, i.e. a HIPIMS mode in which the sputtered atoms satisfy the need for a process gas. Thus no argon or krypton or any other gas is needed (this would eliminate the issues related to noble gas inclusion). Such "gasless" self-sputtering has been demonstrated for HIPIMS using high sputter yield materials such as copper [31]; the HIPIMS pulses were triggered with a short (20 μs) miniature vacuum arc plasmas source. Corresponding experiment with a niobium target did not yield the same result: clearly, the sputter yield of niobium is not sufficient to produce enough "niobium gas". Rather, noble process gas was always needed to obtain HIPIMS pulses.

After this realization we explored the minimum pressure needed to obtain a HIPIMS discharge [32] with niobium. The main result is reproduced in Fig. 7: due to the "left-over plasma" of the previous pulse, the pulse repetition rate was identified as an important parameter that allows us to reduce the pressure yet still operate in a stable, reproducible manner.

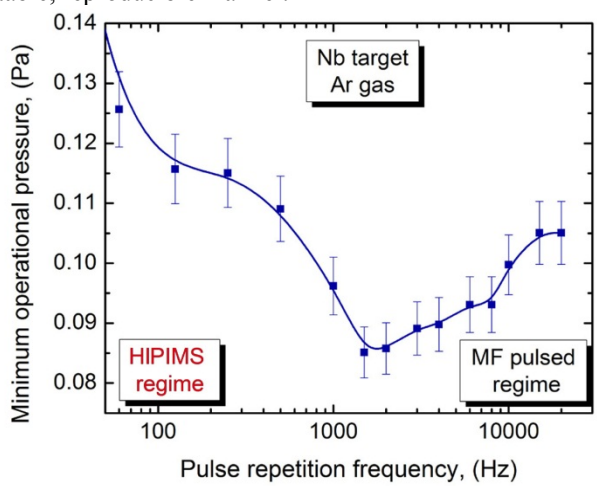

Figure 7: Minimum operational pressure of HIPIMS discharge with 5 cm niobium target in argon; applied voltage 1000 V, pulse length 30 μs, maximum average power 1 kW; for more details see [32].

Moving on from plasma characterization to film deposition, niobium films of typically 1 μm in thickness were deposited on electropolished copper coupons, polished aluminum sheet, aluminum-coated silicon coupons, and glass substrates. Figure 8 shows an optical micrograph of a niobium film deposited on electropolished copper: the film clearly reproduces all defects of the substrates (we checked: the bare substrate exhibits practically the same features). Adhesion on copper is moderate: while not peeling off on its own, the film could be removed by scratching and by the common Scotch Tape test.

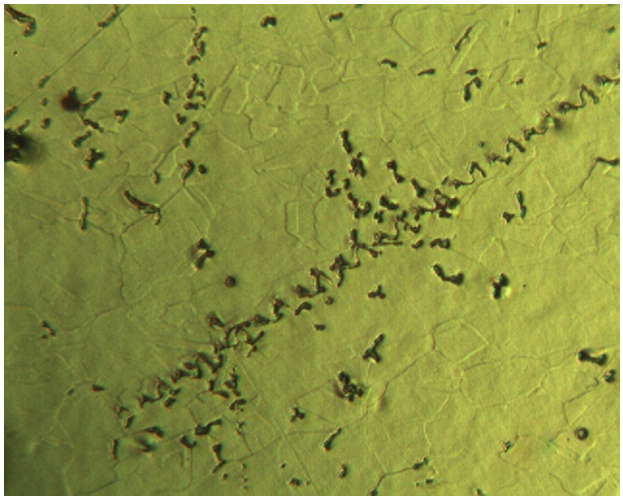

Figure 8: Optical micrograph (width 200 μm) of a rather defective part of a niobium film on electropolished copper: one can see that the film replicates all features of the substrate including grain boundaries and defects.

To emulate deposition on aluminum cavities, polished (4000 grid) aluminum sheet as well as silicon wafers sputtered-coated with aluminum were used. It was assumed that the coated silicon gives a smoother surface and thus most measurements were done on these samples. The aluminum films of about 200 nm were deposited using standard dc magnetron sputtering with the substrate at room temperature. The niobium films were deposited on top after briefly exposing the aluminum surface to an oxygen plasma from a 40 W, (400 V) oxygen glow discharge. Figure 9 shows a measurement of the critical temperature using measuring currents in the range 10^{-6} to 10^{-3} A.

From figure 9 one can derive the RRR value for this sample, which is 4.36, a disappointingly low value. There are several reasons why it is low. First, the niobium is sitting on top of an aluminum film, and therefore the measurement includes the contribution of aluminum and the RRR does not represent the true value for niobium. Second, the deposition was done in the high vacuum general-use chamber, which implies that impurities are gettered by the film. Third, and this is a point realized in hindsight, room temperature aluminum tends to grow in a competitive growth mode, where some crystallites grow much faster than others depending on orientation and other factors. As a result, the Al film is very rough, and Nb grows rather conformally on such rough surface. This is illustrated in figures 10 and 11.

A set of niobium films was deposited by HIPIMS at different growth temperature. As expected, higher growth temperature leads to larger grains and hence narrower x-ray diffraction peaks (Fig. 12).

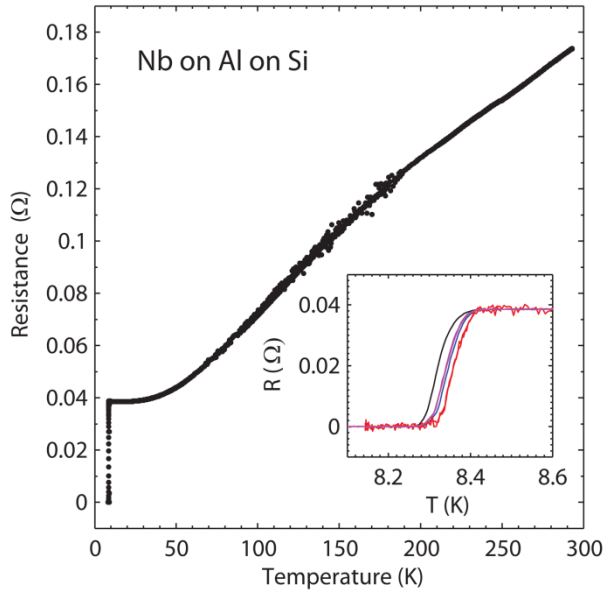

Figure 9: Measurements of the critical temperature of a 1 μm thick niobium film deposited at 400°C on room-temperature-deposited aluminum film on silicon. The inset shows the transition to superconductivity with greater resolution, with the curves taken using different measuring currents.

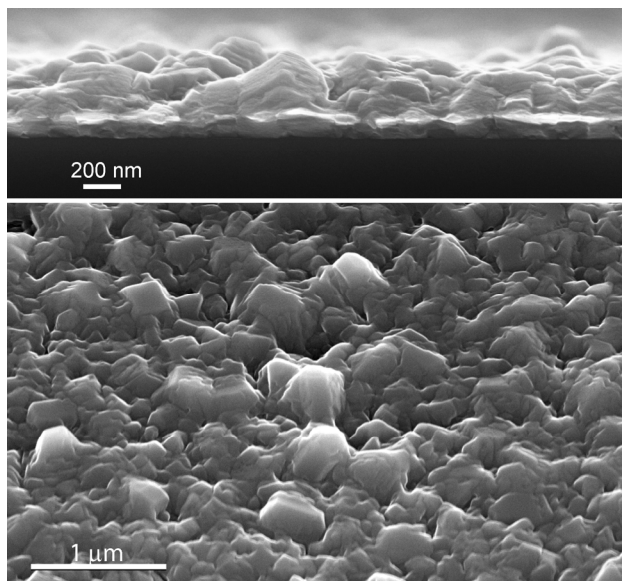

Figure 10: Aluminum layer deposited at room temperature by dc-sputtering: the surprisingly large surface roughness is an issue for the quality of the successively deposited niobium film.

However more information can be extracted from figure 12: elevating the substrate temperature to 200°C did not change the crystallinity very much, whereas elevation to 400°C makes a big difference. A temperature of 400°C appears rather high in light of the melting temperature of aluminum, 660°C. Besides larger crystals, one can also see a shift of the niobium 100 peak toward the bulk position, which can be linked to stress relaxation.

The important role of the substrate is further emphasized when using an amorphous substrate such as glass. The resulting film of niobium is finely grained with a characteristic gain pattern as shown in Fig. 13. Deposition on an insulating substrates was motivated to eliminate a conducting underlayer which distort RRR measurements, however, clearly, the film structure greatly depends on the texture of the substrate.

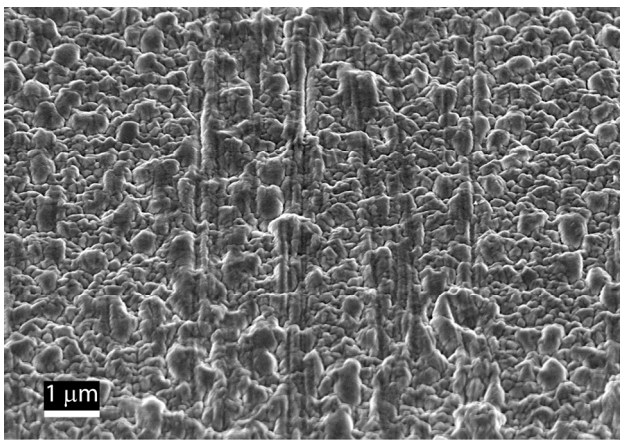

Figure 11: Niobium film of Fig. 9 showing large roughness, as caused by the roughness of the underlayer. Scratches of the substrate are replicated in the film, stressing the importance of proper substrate pretreatment.

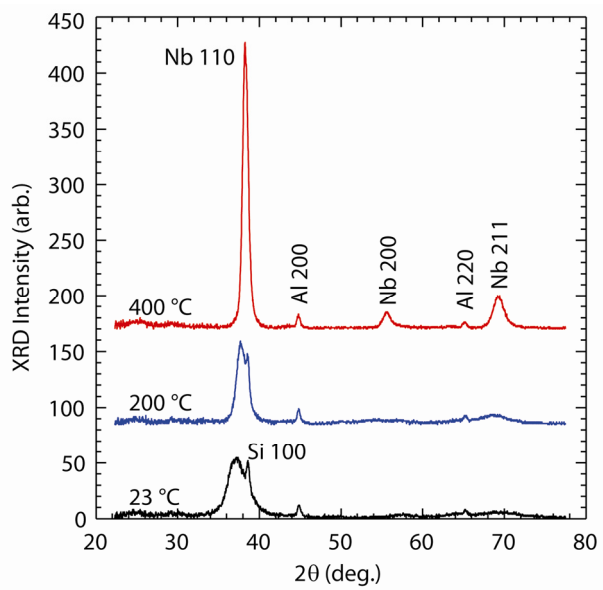

Figure 12: X-ray diffraction patterns for niobium films grown on aluminum films that were deposited by dc magnetron sputtering on silicon at room temperature.

Moving on to the new dual–magnetron HIPIMS system, it was qualified to be operational with a base pressure in the low 10^{-8} Torr, and further improvements may be possible when using the getter effect of an additional niobium magnetron "pump" installed in the same chamber. As with the previous setup, the HIPIMS discharge can ran away to high current levels, and by choosing the applied voltage one can maintain a low or high power mode, which is strikingly obvious just by observing the different colors of the discharge: it is either gas dominated (Fig. 14) or metal dominated (Fig. 15). No films have been grown yet in this system.

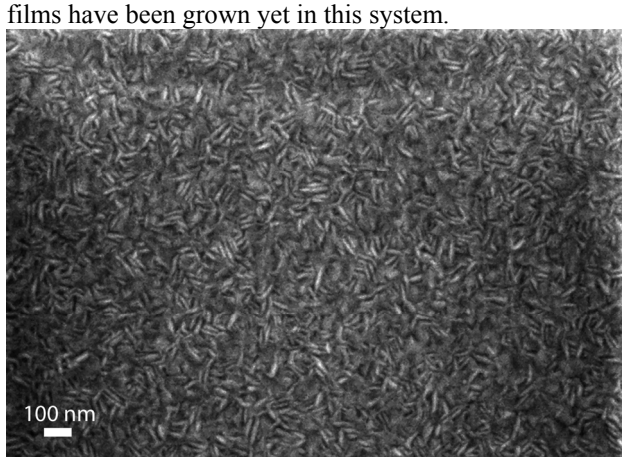

Figure 13: SEM of a niobium film on glass reveals the fine-grained crystalline surface morphology.

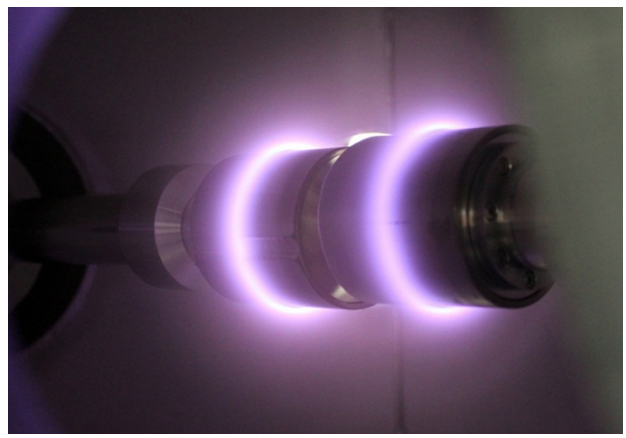

Figure 14: Dual HIPIMS magnetron operating at the relatively low average power of 200 W, with 520 V applied to the target: the light emission is mainly from excited argon.

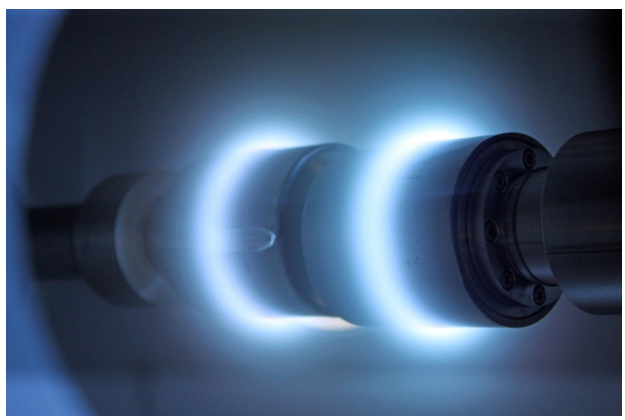

Figure 15: As figure 14 but with the HIPIMS discharge above the runaway threshold; the applied voltage is 760 V, leading to an average power of 550 W and a peak current of 120 A: the light is mainly emitted from niobium. The camera sensor exposure is reduced compared to Fig. 14.

DISCUSSION AND OUTLOOK

The opportunities with the new system are clear: one needs to perform systematic studies on film quality using HIPIMS in a relevant geometry, e.g. using dummy cavities and/or coupons inserted in such dummy cavities, and then proceed to coating on actual SRF cavities. Apart from applying bias, which will be a crucial parameter set on its own, the cavity surface may be *in-situ* plasma-pretreated. The hollow shape of the cavity suggests the use of the hollow cathode effect. This could be a promising approach to optimize an oxide layer which appears to be very important for the adhesion and texture of the coating.

The current dual magnetron setup could be used in several other ways. First, one could add nitrogen and produce NbN, a superconductor on its own with T_c= 16 K, or part of a system with superconducting films [33]. Second, one could use different target materials and adjust the stoichiometry through asymmetric operation in amplitude and pulse width. Niobium-tin (Nb_3Sn) and niobium-titanium alloys are prime candidates. Finally, one could conceivably use the system to follow up on ideas of Gurevich who proposed to use a multilayer coating consisting of alternating insulating layers and thin superconducting layers of thickness smaller than the London penetration depth [34].

REFERENCES

[1] H. Padamsee, J. Knobloch, T. Hays, RF Superconductivity for Accelerators, Wiley-Interscience, New York, 2008.

[2] H. Padamsee, RF Superconductivity: Science, Technology and Applications, Wiley-VCH, Weinheim, 2009.

[3] V. Arbet-Engels, C. Benvenuti, S. Calatroni, P. Darriulat, M.A. Peck, A.M. Valente, C.A. Van't Hof, Nucl. Instrum. Meth. Phys. Res. A 463 (2001) 1.

[4] D. Bloess, Vacuum 47 (1996) 597.

[5] C. Benvenuti, Superconducting coatings for accelerating RF cavities: Past, present, future, Proc. Fifth Workshop on RF Superconductivity, DESY, Hamburg, Germany, 1991, p. 189.

[6] J. Langner, M. Cirillo, W. DeMasi, V. Merlo, R. Sorchetti, R. Russo, S. Tazzari, Modified cylindrical magnetron sputtering system for niobium superconducting film deposition, 5th Int. Conf. on Modification of Materials with Particle Beams and Plasma Flows, Tomsk Polytechnic University and Institute of High Current Electronics, Tomsk, Russia, 2000, p. 399.

[7] E. Bemporad, et al., Superconductor Sci. Technol. 21 (2008) 125026.

[8] J. Langner, R. Mirowski, M.J. Sadowski, P. Strzyzewski, J. Witkowski, S. Tazzari, L. Catani, A. Cianchi, J. Lorkiewicz, R. Russo, Vacuum 80 (2006) 1288.

[9] L. Catani, A. Cianchi, J. Lorkiewicz, S. Tazzari, J. Langner, P. Strzyzewski, M. Sadowski, A. Andreone, G. Cifariello, E. Di Gennaro, Physica C: Superconductivity 441 (2006) 130.

[10] X. Zhao, A.M. Valente-Feliciano, C. Xu, R.L. Geng, L. Phillips, C.E. Reece, K. Seo, R. Crooks, M. Krishnan, A. Gerhan, B. Bures, K.W. Elliott, J. Wright, J. Vacuum Sci. Technol. A 27 (2009) 620.

[11] M. Krishnan, E. Valderrama, C. James, B. Bures, K.W.E.X. Zhao, L. Phillips, B. Xiao, C. Reece, K. Seo, Energetic Condensation Growth of Nb films for SRF Accelerators 4th Int. Workshop on Thin Films and New Ideas for Pushing the Limits of RF Superconductivity, Padua, Italy, 2010.

[12] S. Calatroni, J. Phys.: Conf. Series 114 (2008) 012006.

[13] V. Kouznetsov, K. Macak, J.M. Schneider, U. Helmersson, I. Petrov, Surf. Coat. Technol. 122 (1999) 290.

[14] K. Sarakinos, J. Alami, S. Konstantinidis, Surf. Coat. Technol. 204 (2010) 1661.

[15] A. Anders, Surf. Coat. Technol. 205 (2011) S1.

[16] J. Alami, P.O.A. Persson, D. Music, J.T. Gudmundsson, J. Bohlmark, U. Helmersson, J. Vacuum Sci. Technol. A 23 (2005) 278.

[17] J. Alami, P. Eklund, J.M. Andersson, M. Lattemann, E. Wallin, J. Bohlmark, P. Persson, U. Helmersson, Thin Solid Films 515 (2007) 3434.

[18] A. Anders, Surf. Coat. Technol. 93 (1997) 158.

[19] A. Anders, Cathodic Arcs: From Fractal Spots to Energetic Condensation, Springer, New York, 2008.

[20] D.B. Chrisey, G.K. Hubler (Eds.), Pulsed Laser Deposition of Thin Films, Wiley, New York, 1994.

[21] J.A. Hopwood (Ed.), Ionized Physical Vapor Deposition, Academic Press, San Diego, CA, 2000.

[22] A. Anders (Ed.), Handbook of Plasma Immersion Ion Implantation and Deposition, Wiley, New York, 2000.

[23] A. Anders, J. Vac. Sci. Technol. A 28 (2010) 783.

[24] A. Anders, J. Andersson, A. Ehiasarian, J. Appl. Phys. 102 (2007) 113303.

[25] N. Brenning, R.L. Merlino, D. Lundin, M.A. Raadu, U. Helmersson, Phys. Rev. Lett. 103 (2009) 225003.

[26] S.M. Rossnagel, J. Vac. Sci. Technol. A 6 (1988) 19.

[27] D. Horwat, A. Anders, J. Appl. Phys. 108 (2010) 123306.

[28] J. Bohlmark, J. Alami, C. Christou, A. Ehiasarian, U. Helmersson, J. Vac. Sci. Technol. A 23 (2005) 18.

[29] A.P. Ehiasarian, Y.A. Gonzalvo, T.D. Whitmore, Plasma Processes and Polymers 4 (2007) S309.

[30] O.R. Monteiro, J. Vac. Sci. Technol. B 17 (1999) 1094.

[31] J. Andersson, A. Anders, Appl. Phys. Lett. 92 (2008) 221503.

[32] A. Anders, G.Y. Yushkov, J. Appl. Phys. 105 (2009) 073301.

[33] S. Sakai, P. Bodin, N.F. Pedersen, J. Appl. Phys. 73 (1993) 2411.

[34] A. Gurevich, Appl. Phys. Lett. 88 (2006) 012511.